J Arid Land (2014) 6(1): 105–116
doi: 10.1007/s40333-013-0189-4
jal.xjegi.com; www.springer.com/40333

Characteristics of *Caragana korshinskii* and *Hippophae rhamnoides* stemflow and their significance in soil moisture enhancement in Loess Plateau, China

ShengQi JIAN[1], ChuanYan ZHAO[1*], ShuMin FANG[1,2], Kai YU[3]

[1] State Key Laboratory of Grassland and Agro-Ecosystems, School of Life Sciences, Lanzhou University, Lanzhou 730000, China;
[2] College of Resource and Environmental Sciences, Gansu Agricultural University, Lanzhou 730000, China;
[3] Ministry of Education Key Laboratory of Western China Environmental Systems, Lanzhou University, Lanzhou 730000, China

Abstract: Stemflow of xerophytic shrubs represents a significant component of water replenishment to the soil-root system and influences water utilization of plant roots at the stand scale, especially in water-scarce semi-arid ecosystems. The stemflow of two semi-arid shrubs (*Caragana korshinskii* and *Hippophae rhamnoides*) and its effect on soil moisture enhancement were evaluated during the growing season of 2011 in the semi-arid loess region of China. The results indicated that stemflow averaged 12.3% and 8.4% of the bulk precipitation for *C. korshinskii* and *H. rhamnoides*, respectively. Individual stemflow increased in a linear function with increasing rainfall depth. The relationship between funneling ratios and rainfall suggested that there existed a rainfall depth threshold of 11 mm for both *C. korshinskii* and *H. rhamnoides*. Averaged funneling ratios were 156.6±57.1 and 49.5±30.8 for *C. korshinskii* and *H. rhamnoides*, respectively, indicating that the canopy architecture of the two shrubs was an effective funnel to channel stemflow to the root area, and *C. korshinskii* showed a greater potential to use stemflow water in the semi-arid conditions. For individual rainfall events, the wetting front depths were approximately 2 times deeper in the rooting zone around the stems than in the bare area outside canopy for both *C. korshinskii* and *H. rhamnoides*. Correspondingly, soil water content was also significantly higher in the root area around the shrub stem than in the area outside the shrub canopy. This confirms that shrub stemflow conserved in the deep soil layers may be an available moisture source for plant growth under semi-arid conditions.

Keywords: precipitation; stemflow; funneling ratio; rainfall intensity; Anjiapo catchment

Citation: ShengQi JIAN, ChuanYan ZHAO, ShuMin FANG, Kai YU. 2014. Characteristics of *Caragana korshinskii* and *Hippophae rhamnoides* stemflow and their significance in soil moisture enhancement in Loess Plateau, China. Journal of Arid Land, 6(1): 105–116. doi: 10.1007/s40333-013-0189-4

Water scarcity is the greatest in arid and semi-arid regions because of limited supplies and increasing demand due to greater population growth relative to more humid regions (Leonard, 1961; Carlisle et al., 1966; Cape et al., 1991). Thus, precipitation plays an important role in water-scarce semi-arid environments. The pattern of transferring limited rainfall to the soil will regulate the soil water replenishment and utilization of plant roots. Stemflow is the process that directs precipitation down plant branches and stems. The redirection of water by this process is of ecohydrological and biogeochemical importance in forested and agricultural ecosystems because it is a spatially localized point input of water and nutrients at the plant stem (Enright, 1987). Stemflow has a significant influence on runoff generation, soil erosion, ground water recharge, spatial patterning of soil moisture, soil solution chemistry and the distribution of understory vegetation and epiphytes (Tromble, 1988). Although previous studies paid little attention to the effects of

*Corresponding author: ChuanYan ZHAO (E-mail: nanzhr@lzb.ac.cn)
Received 2012-11-01; revised 2013-04-08; accepted 2013-05-27

stemflow due to the low ratio of stemflow to precipitation reported in many forest stands (Návar and Bryan, 1990; Whitfors et al., 1997; Johnson and Lehman, 2006), the point input characteristic of stemflow may have major implications for soil water dynamics, even for tree species with a low ratio of stemflow to precipitation. Most previous studies on stemflow have been primarily conducted in tropical and temperate forests; in contrast, relatively few studies on stemflow characteristics were documented for shrub vegetation in arid and semi-arid regions (Whitford et al., 1997; Johnson and Lehmann, 2006; Li et al., 2009).

Stemflow could be an important source of soil moisture in arid and semi-arid lands. Aboal et al. (1999) quantified the stemflow of 30 sample trees belonging to six different species in a laurel forest and found that stemflow amount could reach 12.8 times of precipitation in the infiltration areas of the trees, even though the annual stemflow only represented 6.85% of the gross precipitation. Carlyle-Moses (2004) reported that *Flourensia cernua* was capable of channeling approximately 50% of the incident gross precipitation to the plant stem. Návar and Bryan (1990) calculated that the stemflow inputs to the soil area around three semi-arid shrub stems in northeastern Mexico represented a water input that was five times that received by other areas below the shrub canopies. Nulsen et al. (1986) found that the canopy of mallee vegetation intercepts rainwater and redistributes it into soil via stemflow to depths as great as 28 m, and that this stored water is possibly used during the dry summer. Some other arid and semi-arid shrubs are also adapted to divert rainfall to the root zone as stemflow where it subsequently infiltrates the soil and remains available for plant uptake in the deeper soil layer (Pressland, 1973; Nulsen et al., 1986; Návar, 1993; Martinez-Meza and Whitford, 1996; Li et al., 2008).

Except for the factors of forest types and locations, stemflow yield is greatly influenced by meteorological conditions such as rainfall amount, rainfall intensity, wind speed, and wind direction (Crockford and Richardson, 1990; Levia and Frost, 2003). Although Levia and Frost (2003) pointed out general tendencies of stemflow yield, which increased with the magnitude of a precipitation event and wind speed but decreased with rainfall intensity of incident gross precipitation, they also presented some study cases that contrasted with generally held assumptions, exemplifying the diverse relationship between stemflow yield and meteorological conditions. The amount and timing of stemflow are mainly determined by meteorological conditions and stem and branch architecture. Stemflow values are highly variable with different climate types. Levia and Frost (2003) reported stemflow values of approximately 3.5%, 11.3% and 19% of the bulk precipitation for tropical, temperate, and semi-arid regions, respectively. For the shrub species, relative stemflow decreases with increasing annual rainfall, and percentages differ strongly by species (Llorens and Domingo, 2007). Stemflow is high in some species, such as *Rosmarinus officinalis* (42.5%) and *Thymus vulgaris* (31%) under very dry conditions (Belmonte and Romero, 1998), and low, between 4% and 7% of annual rainfall, in others, like *Adenocarpus decorticans*, *Retama sphaerocarpa* and *Cistus laurifolius* (Levia and Frost, 2003). Therefore, it is necessary to study stemflow characteristics for various shrub species, which is important for an accurate representation of parameters of stemflow fluxes in hydrological models (Llorens and Domingo, 2007).

In China, little work has been done on stemflow for shrub vegetation in arid and semi-arid regions, where the establishment of vegetation is quite difficult due to inadequate availability of moisture. The objectives of this study were to (1) determine the influence of two dominant shrub types (*Caragana korshinskii* and *Hippophae rhamnoides*) and rainfall characteristics (depth and intensity) on stemflow production and funneling ratios; and (2) assess the impact of stemflow on soil moisture status in the semi-arid loess region of China.

1 Materials and methods

1.1 Study area

The study was conducted from June to October of both 2011 and 2012 at the Anjiapo catchment, Dingxi county (35°35′N, 104°39′E) of Gansu province in western Chinese Loess Plateau. The mean annual pre-

cipitation is 420 mm with great inter-annual variations. Over 60% of the precipitation falls between July and September and over 50% of it occurs with storms. The monthly average air temperature ranges from –7.4°C to 27.5°C, with an annual mean temperature of 6.3°C. Average annual pan evaporation is 1,510 mm. The predominant gray calcareous soil developed on loess parent materials with silt texture has a relatively high thickness.

The study area is a loess region covered by sparse vegetation of species such as *Pinus tabuliformis*, *Populus tomentosa*, *Prunus armeniaca*, *Robinia pseudoacacia*, *C. korshinskii* and *H. rhamnoides*. *C. korshinskii* is a perennial medium shrub with a height of 0.5–2.0 m; while *H. rhamnoides* is a deciduous shrub with a main stem and narrow but thin leaves. They vary in traits such as aboveground growth rates, canopy height, rooting depth and so on. The description and characteristics of our experimental sites are presented in Table 1.

Table 1 A brief view of the areas of survey for *C. korshinskii* and *H. rhamnoides*

Species	Aspect	Slope (°)	Slope position	Age of stand (a)
C. korshinskii	SE	15	Middle	10
H. rhamnoides	N	19	Upper	11

1.2 Stemflow determination

Stemflow was measured for 16 plant species representing the two dominant shrubs in the study area. The 16 plant species comprised 8 individuals of *C. korshinskii* and *H. rhamnoides*, respectively. For the stemflow collection, fine sand paper was used to burnish the selected branch surface about 10 cm above the ground. Then, stemflow was collected using collars constructed from flexible aluminum foil plates that were fitted around the entire circumference of the branches. Each collar was sealed to the branch using all weather silicon caulking. Stemflow water was delivered from the collar to a collection bottle via a 1-cm aperture plastic hose. Stemflow was measured by a graduated cylinder for each branch after each rainfall event and summarized for a single shrub. The stemflow volume of each shrub was divided by its canopy area to calculate the stemflow depth on a stand basis (Li et al., 2008).

1.3 Canopy structure determination

Canopy variables that were measured on each shrub included: shrub height, basal diameter, branch angle, the height between the base and first branch (HBB), projected area, and canopy bulk. Shrub height was measured at the centre of the canopy. Basal diameter was calculated with collar girth at the base. Projected area was determined by taking the east-west and north-south diameters through the centre of the fullest part of the canopy. Canopy bulk was obtained by using the formula for an inverted cone, while stem length was regarded as the sum of the total branch length. A standard rain gauge and a siphon-type recording rain gauge were used to obtain the amount and intensity of rainfall.

The surface water storage capacity of each type of plant cover is an essential contributor to stemflow process. The water storage capacity was determined by immersion. Freshly cut shrubs were immersed whole in water following a procedure similar to that described in Wood et al. (1998).

1.4 Funneling ratio determination

Herwitz (1986) suggested that the quantitative importance of stemflow at the point scale can be expressed as a funneling ratio, F:

$$F = V/(B \times P). \quad (1)$$

Where V is the stemflow volume (L), B is basal area of the shrub (m^2), and P is the incident rainfall at the top of the canopy (mm).

The product $B \times P$ provides the volume of water that would have been caught by a rain gauge having an opening equal to that of the tree basal area. Thus, F represents the ratio of the amount of precipitation delivered to the base of the tree to the rainfall that would have reached the ground if the tree were not present. Funneling ratios of >1 indicate that canopy components other than the tree bole are contributing to stemflow (Herwitz, 1986; Carlyle-Moses and Price, 2006).

1.5 Wetting front and soil moisture determination

Another three plant species for each shrub species were selected to assess the effect of stemflow on soil moisture recharge. Using TRIME-FM time domain

reflectometry (TDR) (Campbell, CS-610), soil water contents around the stem and at about 30 cm from the plant periphery in the bare area were measured to a depth of 100 cm with sampling increment of 10 cm after several rainfall events characterized by high, medium and low intensities. Wetting front depths within soil were also recorded to detect stemflow advancement patterns.

1.6 Dye tracing

Two plants for each shrub were selected to conduct dye stained and infiltration tests. Brilliant Blue FCF was chosen because it has a relatively low toxicity, low sorption and high mobility. The low sorption and high mobility properties were important because the dye was required to travel through the soil. Brilliant Blue FCF dye was added to the test water at a concentration of 4.0 g/L. We tied up the plastic bottles filled with solution to the stem, and then stabbed a small hole in the contact position. The solution infiltrated into the soil along the stem. Excavations were conducted to map soil features and examine flow patterns for each of the dye stained tests. Soil sections were carefully cut using hand tools to reduce damage to soil structure, and photographed with a digital camera using procedures adapted from Forrer et al. (2000) and an opaque tarp to diffuse sunlight. Image processing was conducted using ERDAS IMAGINE version 9.2 and ArcGIS 9.3 geographic software. Image analysis procedures developed by Weiler and Flühler (2004) and Forrer et al. (2000) were used with selected modifications to improve examination of dye stained patterns and to ensure consistency between images. A detailed description of the image analysis procedures was provided in Cey and Rudolph (2009). Images were processed by the following steps: geometric correction, background subtraction, color adjustment, histogram stretching, dye classification, and a final visual check. This process classified areas as either unstained or stained.

2 Results

2.1 Rainfall characteristics during the experimental period

There were a total of 47 rainfall events in 2011, resulting in an annual precipitation of 226.1 mm with an average rainfall intensity of 2.82 mm/h (ranging from 0.1 to 32.5 mm/h) and an average individual rainfall amount of 9.1 mm (ranging from 0.1 to 27.3 mm) (Fig. 1). Stemflow was monitored during 22 of the 47 rainfall events. The 22 events produced 202.3 mm of rainfall, which accounted for 89.5% of the annual rainfall amount. The maximum rainfall intensity in 10 min (I_{10}) ranges from 0.8 to 31.0 mm/h. In order to facilitate the analysis, the rainfall events were divided into six classes (Table 2).

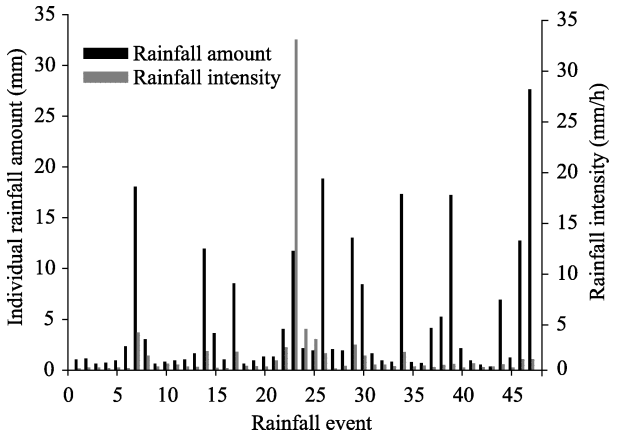

Fig. 1 Rainfall amount and rainfall intensity for 47 individual rainfall events in the study area during 2011

Table 2 Rainfall characteristics of the study area during the experimental period

Rainfall class (mm)	Rainfall frequency	Frequency percentage (%)	Rainfall amount (mm)	Rainfall percentage (%)	Rainfall intensity (mm/h)
<2	17	36.2	15.1	5.6	0.50
2–5	11	23.4	33.7	12.6	1.65
5–10	8	17.0	61.1	22.9	1.27
10–15	7	14.9	82.5	30.9	
15–20	3	6.4	47.6	17.8	1.44
>20	1	2.1	27.3	10.2	

2.2 Funneling ratios

Figure 2 shows the relationship between funneling ratio (F) and rainfall depth for *C. korshinskii* and *H. rhamnoides*. Results indicate a systematic pattern of funneling ratios in which the rainfall depth first increased until a threshold value of 11 mm and then the F values tended to be stable for both species. Average

funneling ratio was 156.1, 62.2, and ranged from 27.3 to 274.2, 18.5 to 184.9 for *C. korshinskii* and *H. rhamnoides*, respectively.

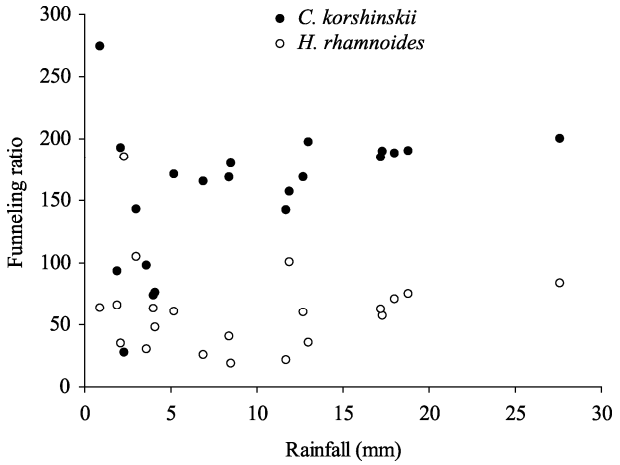

Fig. 2 Relationship between funneling ratio and rainfall for *C. korshinskii* and *H. rhamnoides*

2.3 Stemflow characteristics

2.3.1 Canopy structure and stemflow

The stemflow values showed positive correlation with projected area, height, branch number and canopy bulk for *C. korshinskii* and *H. rhamnoides*, respectively (Table 3). The larger specimens were able to obtain more stemflow than the smaller shrubs, and for similar canopy surface areas, stemflow water increased with deceasing branch angle. No correlation was detected between stemflow and HBB and basal diameter.

Stepwise regression equation of stemflow with the canopy structures was as Eq. 2 (Aboal et al., 1999).

$$SF_{vol}=0.001X_1-0.656X_2+43.829,\ R^2=0.879,\ F=26.469,\ \text{Sig.}=0.002. \quad (2)$$

Where, SF_{vol}, stemflow volume (mL); X_1, projected area (m^2); X_2, branch angle (°).

The equation contains two independent variables and indicates that stemflow increases with the increase in the projected area and the decrease in the branch angle, suggesting that stemflow is governed by projected area and branch angle.

2.3.2 Rainfall characteristics and stemflow

Figure 3a shows that individual stemflow was strongly correlated with individual rainfall. Stemflow increased with increasing rainfall depth and followed a positive linear function. Large variability in stemflow percentage was found for rainfall depth of less than 6 mm and stemflow percentage tended to be stable with increasing rainfall depth. The stable values were 13.71% and 4.55% for *C. korshinskii* and *H. rhamnoides*, respectively. *C. korshinskii* showed a power correlation between stemflow percentage and rainfall depth, and *H. rhamnoides* had the exponential distribution (Fig. 3b).

There was a weaker correlation between stemflow percentage and mean rainfall intensity. It may be due to the non-uniform distribution of rainfall during the rainfall period. The mean rainfall intensity cannot well represent the actual rainfall intensity. The relationship between the maximum rainfall intensity in 10 minutes (I_{10}) and stemflow was presented (Fig. 4). Large variability in stemflow percentage was found for I_{10} of less than 6 mm/h and stemflow percentage tended to be stable with increasing I_{10}. The stable values were 12.66% and 2.89% for *C. korshinskii* and *H. rhamnoides*, respectively.

Multiple regression equations of stemflow with the rainfall amount, mean rainfall intensity and I_{10} in Table 4 indicated that stemflow increased by 2.6%–8.0%

Table 3 Correlation coefficients between stemflow and canopy structure morphology of two shrub species

Items	Mean		*r*	
	C. korshinskii	*H. rhamnoides*	*C. korshinskii*	*H. rhamnoides*
Projected area (m^2)	3.02	1.61	0.87^{**}	0.79^{**}
Height (m)	1.75	1.54	0.61^{ns}	0.59^{*}
HBB (m)	0.80	0.47	-0.43^{ns}	-0.21^{ns}
Basal diameter (cm)	1.50	4.70	-0.65^{ns}	-0.47^{ns}
Branch number	19.00	4.00	0.84^{**}	0.89^{**}
Branch angle (°)	59.00	55.00	-0.80^{*}	-0.37^{*}
Canopy bulk (m^3)	4.37	3.01	0.86^{**}	0.91^{**}

Note: HBB, height between the base and first branch; *, $P<0.05$; **, $P<0.01$; ns, not significant.

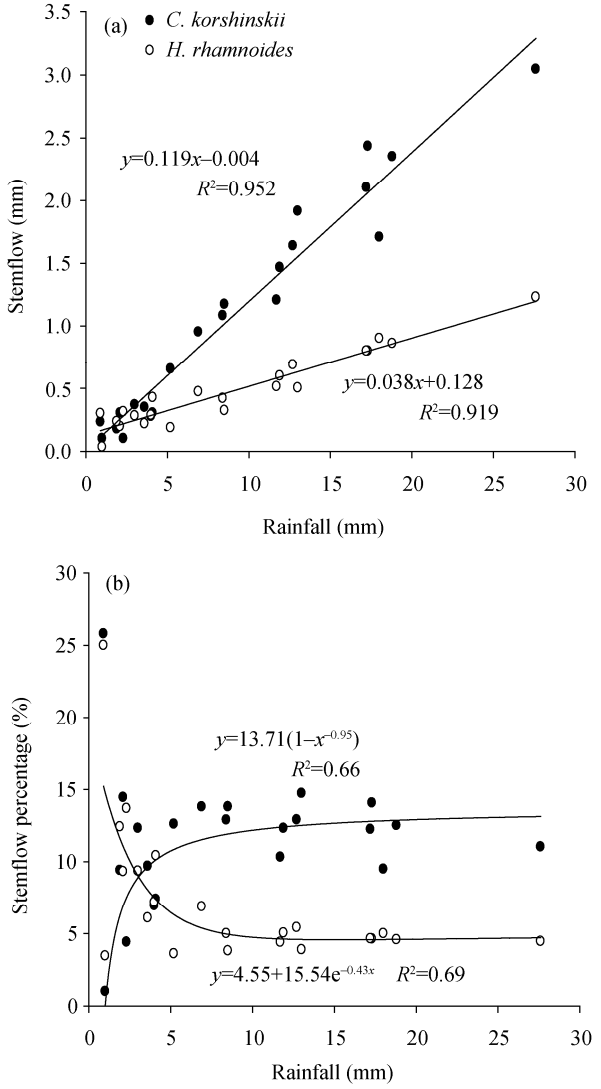

Fig. 3 Relationship between rainfall, stemflow and stemflow percentage

and 0.5%–4.3% with the increase in rainfall and I_{10}, respectively, but by 0.4%–3.2% with the decrease in mean rainfall intensity, suggesting that stemflow was more governed by rainfall amount than by mean rainfall intensity and I_{10} for the two shrub species.

2.4 Wetting front and soil moisture

Stemflow can be channeled to deeper levels of the soil beneath shrubs than at sites away from the shrubs, creating useful concentrations of water in the root zone. Figure 5 shows the wetting front depth of rainwater for two individual rainfall events (11.7 mm and 18.7 mm, respectively). Wetting front depths in the soil around the stem in the root area was approximately 2 times deeper than that in the bare area outside the canopy for both *C. korshinskii* and *H. rhamnoides*. This confirms that stemflow is conducive to the concentration and storage of water in deep layers in the soil profile, indicating that stemflow creates favorable soil water conditions for plant growth.

Figure 6 shows the soil water content on 31 July 2011 in the soil around the stem, beneath the canopy and outside the canopy for *C. korshinskii* and *H. rhamnoides*, respectively after 15.7 mm of rainfall. Soil water content showed less variability at 0–20 cm soil depth. With the deepening of soil depth, soil water content was higher in the soil around the stem than beneath the canopy and outside the canopy for *C. korshinskii* and *H. rhamnoides*, respectively. Paired-Samples *T*-test indicated that average soil water content at 0–100 cm soil depth was 10.4%±14.5% and 10.0%±10.6% significantly higher in the soil around the stem than outside the canopy for *C. korshinskii* and *H. rhamnoides*, respectively.

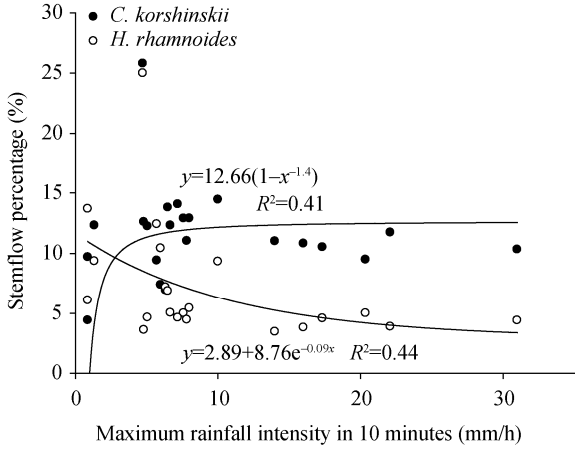

Fig. 4 Relationship between the maximum rainfall intensity in 10 minutes and stemflow percentage

Table 4 Regression equations and coefficient values among stemflow, amount, average intensity and I_{10} of rainfall

Species	Equation	*r*	*F* value	*P*
C. korshinskii	SF= –0.131+0.08P–0.032I+0.043I_{10}	0.877	42.58	<0.0001
H. rhamnoides	SF= –0.149+0.026P–0.004I+0.005I_{10}	0.701	29.02	<0.0001

Note: SF, stemflow (mm); P, rainfall amount (mm); I, rainfall intensity (mm/h); I_{10}, maximum rainfall intensity in 10 minutes (mm/h); r, correlation coefficient.

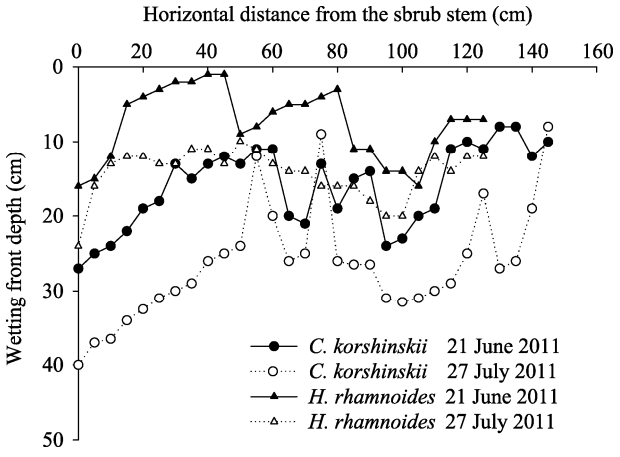

Fig. 5 The change of wetting front depths around the shrub stem for *C. korshinskii* and *H. rhamnoide*

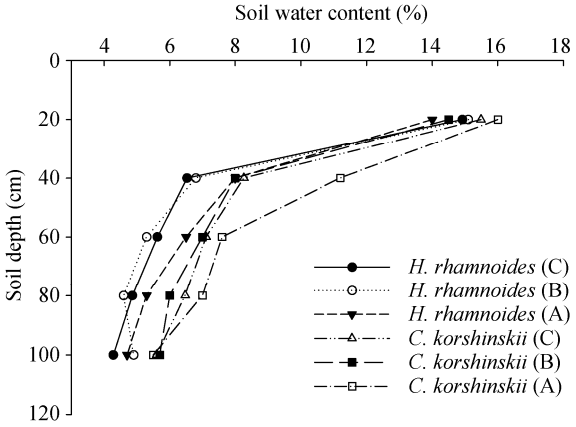

Fig. 6 Soil water content distribution in the soil profile around the shrub stem (A), beneath the canopy (B), and outside the canopy (C)

2.5 The redistribution of stemflow in the soil

Photos stained with Brilliant Blue for different soil depths were selected to qualitatively explain the soil water flow pattern and the characteristics of stemflow in the soil (Fig. 7). In the 0–10 cm soil layer, the conventional tillage and other management measures related to the soil surface resulted in a loose and porous soil structure. At the soil depth of 10–15 cm, macropore flow induced by cracks occurred. Soil at 15–20 cm deep showed poor permeability and lateral flow occurred most likely due to compaction by farm machinery and the presence of plow pan, and below 20 cm, the soil was less disturbed when compared with upper layers, indicating various pore sizes with good continuity. Macropore flow was also generated in this layer. The maximum depths the dye reached were 40 and 35 cm for *C. korshinskii* and *H. rhamnoides*, respectively, and there was significant difference between the two maximum stained depths. The red area indicates the macropore flow paths, which were heavily stained by Brilliant Blue as water infiltrated the soil. The green area indicates the interaction between macropores and the surrounding soil matrix. The red stained area reveals the degree of macropore flow paths and the connectivity of vertical macropore flow paths.

The distribution of the dye stained area as a function of soil depth (Fig. 8) indicates that flow occurred

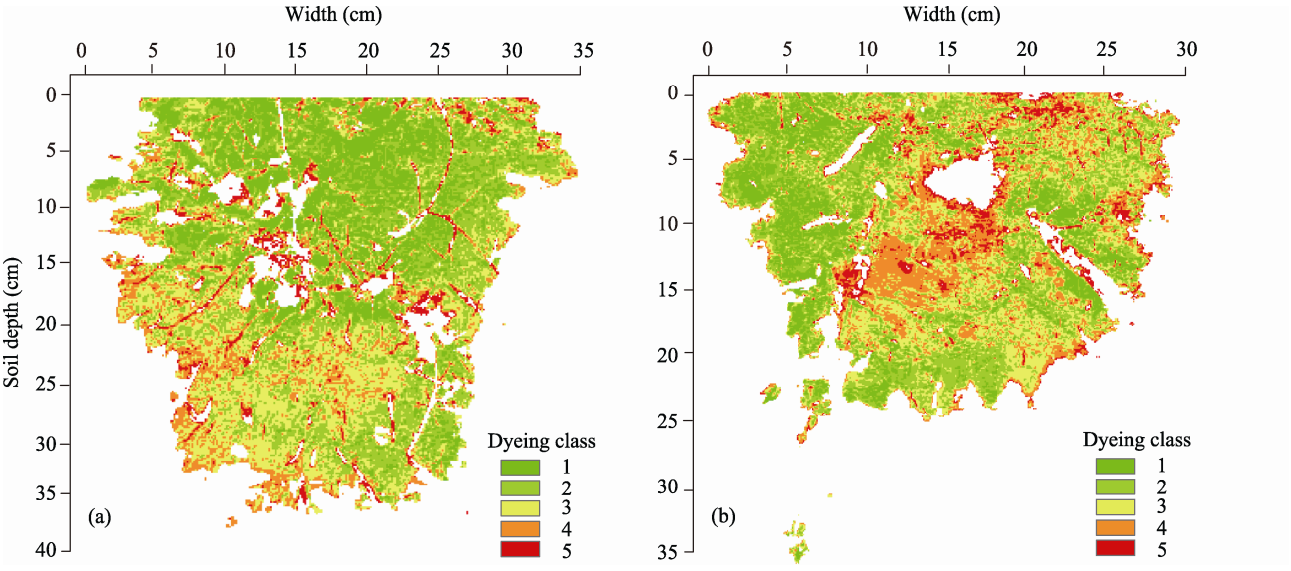

Fig. 7 Computer-enhanced photos of dye stained areas in the vertical soil profiles for *C. korshinskii* (a) and *H. rhamnoides* (b)

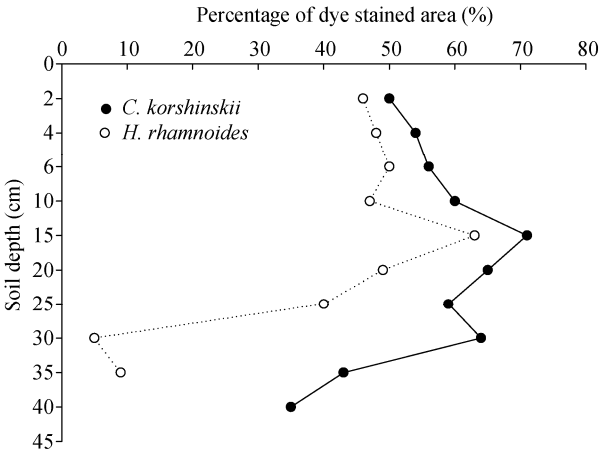

Fig. 8 The change in percentages of dye stained area with soil depth for *C. korshinskii* and *H. rhamnoides*

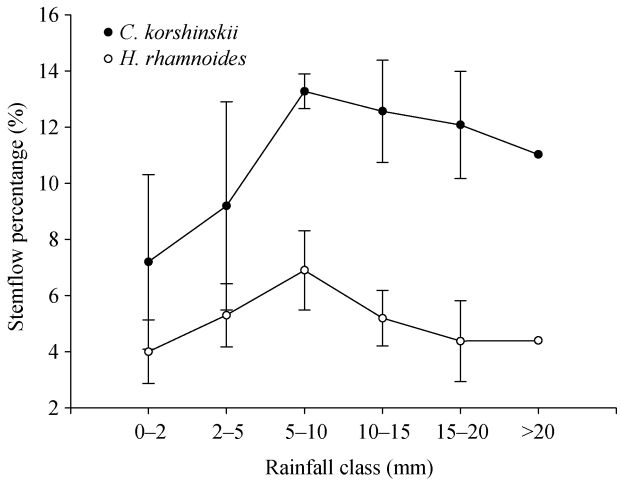

Fig. 9 Relationships between stemflow percentages for two shrub species and rainfall class. Mean±SD.

as water infiltrated the soil, which corresponds with visual observation of soil sections stained using Brilliant Blue. The dye stained area initially increases, then gradually decreases with soil depth after reaching its maximum area. Combination of the macropore flow patterns of longitudinal soil sections indicates that lateral flow results in the largest dye stained area at a depth of 15 cm for *C. korshinskii* and *H. rhamnoides*, respectively. The dye stained area was significantly different between *C. korshinskii* and *H. rhamnoides*, and higher infiltration rates resulted in more longitudinal and lateral flow which occurred for *C. korshinskii*.

3 Discussion

The cumulative stemflow depth during the study period averaged 25.7 and 17.6 mm for *C. korshinskii* and *H. rhamnoides*, respectively. However, being expressed as a percentage of gross rainfall, stemflow in *C. korshinskii* and *H. rhamnoides* averaged 12.3% and 8.4%, respectively. The rainfall was divided into six classes: 0–2, 2–5, 5–10, 10–15, 15–20, >20 mm. Figure 9 shows the stemflow percentages for different rainfall classes. There was a great variability in stemflow percentages among different rainfall classes for *C. korshinskii* and *H. rhamnoide*, respectively. *C. korshinskii* and *H. rhamnoide* indicate a systematic pattern of stemflow percentages first increasing until a threshold value of 5–10 mm and then beginning to decline.

It is suggested that *C. korshinskii* has higher efficiency of stemflow production than *H. rhamnoides*. The relative high efficiency of *C. korshinskii* in producing stemflow is most probably a consequence of the smooth bark associated with this species. *C. korshinskii* is a thorny shrub with small striped or linear leaves, forming a smoother "funnel" to channel stemflow. Herwitz (1985) reported that the water storage capacity associated with smooth bark had been shown to be considerably less than that of rough bark in an Australian rainforest. Comparisons of stemflow production have shown that smooth bark species often generate stemflow under smaller rainfall inputs and that trees produce more stemflow than their rough bark counterparts (Voigt and Zwolinski, 1964; Crockford and Richardson, 1990; Liu, 1998). In contrast, *H. rhamnoides* has numerous thin and densely leaved short branches with grayish glumes, and leaves are short and bulbous scaly. The relative rough bark and small leaves in *H. rhamnoides* may absorb and retain more rainwater, therefore resulting in greater water storage capacity and lower stemflow production (Ford and Deans, 1978; Bui and Box, 1992). In the study, water storage capacities were measured by regression analysis method in whole plants and then by immersing each component (branches, leaves, and trunks) separately in water (Pereira et al., 2009). There were some differences among the two methods due to the effects of different factors. The regression analysis method was mainly impacted by the measurement of

throughfall and leaf area index (LAI) with the maximum water storage capacity of 0.68 mm and 0.72 mm for *C. korshinskii* and *H. rhamnoides*, respectively. The immersion method was mainly impacted by the canopy structure with the maximum water storage capacity being estimated to be 0.73 mm and 0.76 mm for *C. korshinskii* and *H. rhamnoides*, respectively. The immersion method showed that the maximum water storage capacity per unit area of the canopy components was in the order of branches (0.31 mm) > leaves (0.27 mm) > trunks (0.15 mm) for *C. korshinskii*, and trunks (0.33 mm) > branches (0.29 mm) > leaves (0.14 mm) for *H. rhamnoides* (Fig. 10).

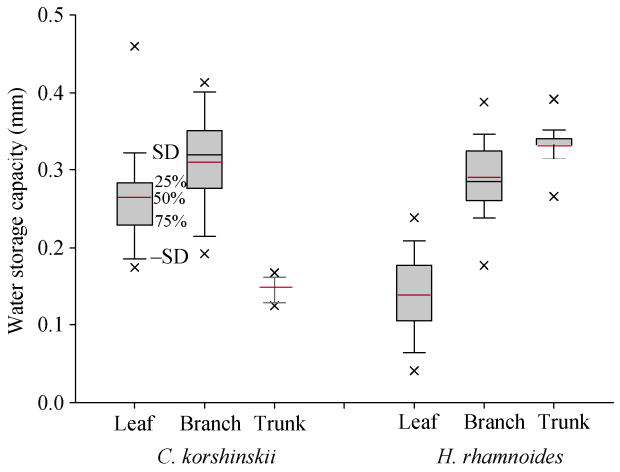

Fig. 10 Box-and-whisker diagrams showing the median, 25th, 50th, 75th percentiles and standard deviation for water storage capacity of each component of *C. korshinskii* and *H. rhamnoides*. The red line is the mean value, (—) the maximum and minimum values, and (×) the 1st and 99th percentiles.

Stemflow for the two shrubs increased as a function of rainfall amount on a rainfall-event basis, which has also been documented by other researchers (Pressland, 1976; Nulsen et al., 1986; Návar, 1993; Martinez-Meza and Whitford, 1996). While the relationship between stemflow percentages and rainfall intensity showed a different trend: first, large variability in stemflow percentages; then an intensity threshold value of 6 mm/h; and finally stability. This may be explained by the following possible reasons: (1) During low intensity rainfall events, most of the initial rainfall was intercepted by the canopy. With increasing rainfall input, a greater proportion of the shrub becomes saturated and thus the area contributing to stemflow increases until a threshold rainfall input that saturates all areas capable of producing stemflow is reached (Llorens and Gallart, 2000). Therefore, stable values exist between stemflow percentages and I_{10} when rainfall intensity is greater than 6 mm/h. (2) Higher intensity rainfalls would result in increased flow velocities along branches that may exceed the flow capacities of those branches.

The funneling ratio varied greatly for different rainfall events, depending on the rainfall amount and rainfall intensity. Funneling ratios have been found to be greater than 10, and in some cases, far greater than 10 (Durocher, 1990; Návar and Bryan, 1990). Our studies showed that there can be ten or even a hundred times the rainwater amount that may reach the root area by stemflow as compared to an open area. The excess water effectively enhances the moisture of the upper soil layer, and then a greater water potential gradient is formed between the upper wet soil layer and the deeper dry soil profile. Consequently, the probability of water infiltrating to the deeper soil becomes higher around shrub stems. Also, stemflow water in semi-arid shrubs may be assumed to be distributed to a deep soil layer by preferential flow along root channels (Gómez et al., 2002). Stemflow water can effectively refill the soil profile and increase the cumulative infiltration for medium and large rainfall events. Stemflow inputs depend not only on rainfall characteristics (such as rainfall amount, intensity, and duration), but also on meteorological conditions, seasonality, and shrub canopy structure. On the other hand, there are interspecific and intraspecific differences among and within shrub species (Wang et al., 2008). Infiltration is also influenced by soil surface characteristics (such as microtopography, cracking, surface sealing, and crusting), soil physical properties (such as bulk density, organic matter, and particle size distribution), and characteristics of the vegetation (such as plant biomass and cover) (Wang et al., 2007).

Funneling ratios all are larger than 1 for *C. korshinskii* and *H. rhamnoides*, indicating that branches and stems were fully contributing to stemflow generation (Návar, 1993). Relatively larger values of funneling ratios for *C. korshinskii* suggest that *C. korshinskii* was most effective for stemflow production, which

resulted in more water that could be conserved into the deep layers of the soil. Deeper wetting fronts and higher water contents in the root area around the two shrub species than those in the area outside the shrub canopy in the study suggest that shrub stemflow can be an available moisture source for plant growth under arid conditions and that water redistribution by shrubs can be considered an essential property of the plants that contributes to the stability of shrub communities in harsh environments (Voigt, 1960). We can get a preliminary understanding about the redistribution of stemflow water in the soil by the method of combining the dye tracer technique with image processing.

The depth of wetting front, soil moisture, and pattern of dye stained area are sensitive to antecedent soil water content and topographic conditions (Durocher, 1990). Figure 11 showed the antecedent soil water content of different experiments. The antecedent soil water content of *H. rhamnoides* at soil depth 0–100 cm was significantly higher than that of *C. korshinskii* for the two different experiments, respectively. The antecedent soil water content showed a similar trend for *C. korshinskii* and *H. rhamnoides*. The soil surface had the lower soil water content and the highest soil water content occurred at a depth of 40 cm.

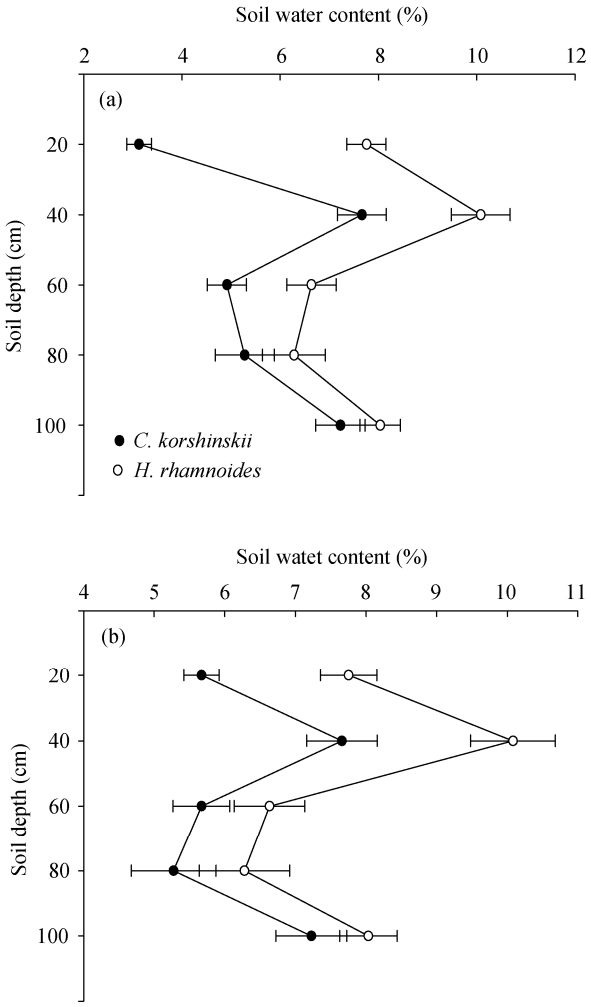

Fig. 11 The antecedent soil water contents of different experiments (a, the antecedent soil water content of wetting front determination; b, the antecedent soil water content of dye tracing experiment). Mean±SD.

4 Conclusion

A better understanding of the stemflow variability and its contribution to soil moisture is essential in semi-arid regions. Owing to the high values of funneling ratios of the studied species, the shrub plants can concentrate water flux to the stem basal area. Thus, from the point view of the funneling ratio and cumulative infiltration, we may conclude that especially for the studied area, where rainfall events are typically small and of low intensity, stemflow is of immense importance to sustain the ecosystem close to and around shrubs at the stand scale. Due to the fact that the structural properties of shrubs and the surface characteristics of their leaves provide the potential for deposition and accumulation of dust and dry fall onthe leaf surfaces, stemflow could transport those materials to the soil under the shrub, contributing to the development of 'fertile islands' under shrub canopies. Higher values of funneling ratios for *C. korshinskii* and *H. rhamnoides* imply that stemflow in the two shrub species can also be an available nutrient source for plant growth under semi-arid conditions.

Acknowledgements

This project was supported by the National Natural Science Foundation of China (91025015, 51178209).

References

Aboal J R, Morales D, Hernandez M, et al. 1999. The measurement and modelling of the variation of stemflow in a laurel forest in Tenerife, Canary Islands. Journal of Hydrology, 221(3–4): 161–175.

Adams M, Angradi T. 1996. Decomposition and nutrient dynamics of

hardwood leaf litter in the Fernow whole-watershed acidification experiment. Forest Ecology and Management, 83(1–2): 61–69.

Belmonte S F, Romero D A. 1998. A simple technique for measuring rainfall interception by small shrub: "interception flow collection box". Hydrological Processes, 12(3): 471–481.

Bui E N, Box J E. 1992. Stemflow, rain throughfall, and erosion under canopies of corn and sorghum. Soil Science Society of America Journal, 56(1): 242–247.

Cape J N, Brown A F H, Robertson S M C, et al. 1991. Interspecies comparisons of throughfall and stemflow at three sites in northern Britain. Forest Ecology and Management, 46(3–4): 165–177.

Carlisle A, Brown A H F, White E J. 1966. The organic matter and nutrient elements in the precipitation beneath a sessile oak (*Quercus petraea*) canopy. The Journal of Ecology, 54(1): 87–98.

Carlyle-Moses D E. 2004. Throughfall, stemflow, and canopy interception loss fluxes in a semi-arid Sierra Madre Oriental matorral community. Journal of Arid Environments, 58(2): 181–202.

Carlyle-Moses D E, Price A G. 2006. Growing-season stemflow production within a deciduous forest of southern Ontario. Hydrological Processes, 20(17): 3651–3663.

Crockford R H, Richardson D P. 1990. Partitioning of rainfall in a eucalypt forest and pine plantation in southeastern Australia: II Stemflow and factors affecting stemflow in a dry sclerophyll eucalypt forest and a Pinus radiata plantation. Hydrological Processes, 4(2): 145–155.

Durocher M G. 1990. Monitoring spatial variability of forest interception. Hydrological Processes, 4(3): 215–229.

Enright N J. 1987. Stemflow as a nutrient source for nikau palm (*Rhopalostylis sapida*) in a New Zealand forest. Australian Journal of Ecology, 12(1): 17–24.

Ford E D, Deans J D. 1978. The effects of canopy structure on stemflow, throughfall and interception loss in a young Sitka spruce plantation. Journal of Applied Ecology, 15(3): 905–917.

Forrer I, Papritz A, Kasteel R, et al. 2000. Quantifying dye tracers in soil profiles by image processing. European Journal of Soil Science, 51(2): 313–322.

Gómez J A, Vanderlinden K, Giraldez J V, et al. 2002. Rainfall concentration under olive trees. Agricultural Water Management, 55(1): 53–70.

Herwitz S R. 1985. Interception storage capacities of tropical rainforest canopy trees. Journal of Hydrology, 77(1–4): 237–252.

Herwitz S R. 1986. Infiltration-excess caused by stemflow in a cyclone-prone tropical rainforest. Earth Surface Processes and Landforms, 11(4): 401–412.

Herwitz S R. 1987. Raindrop impact and water flow on the vegetative surfaces of trees and the effects on stemflow and throughfall generation. Earth Surface Processes and Landforms, 12(4): 425–432.

Jabro J D, Lotse E G, Simmons K E, et al. 1991. A field study of macropore flow under saturated conditions using a bromide tracer. Journal of Soil and Water Conservation, 46(5): 376–380.

Johnson M S, Lehmann J. 2006. Double-funneling of trees: stemflow and root-induced preferential flow. Ecoscience, 13(3): 324–333.

Leonard R E. 1961. Net precipitation in a northern hardwood forest. Journal of Geophysical Research, 66(8): 2417–2421.

Levia D F, Frost E E. 2003. A review and evaluation of stemflow literature in the hydrologic and biogeochemical cycles of forested and agricultural ecosystems. Journal of Hydrology, 274(1–4): 1–29.

Li X Y, Liu L Y, Gao S Y, et al. 2008. Stemflow in three shrubs and its effect on soil water enhancement in semiarid loess region of China. Agricultural and Forest Meteorology, 148(10): 1501–1507.

Li X Y, Yang Z P, Li Y T, et al. 2009. Connecting ecohydrology and hydropedology in desert shrubs: stemflow as a source of preferential flow in soils. Hydrology and Earth System Sciences, 13: 1133–1144.

Liu S. 1998. Estimation of rainfall storage capacity in the canopies of cypress wetlands and slash pine uplands in North-Central Florida. Journal of Hydrology, 207(1–2): 32–41.

Llorens P, Gallart F. 2000. A simplified method for forest water storage capacity measurement. Journal of Hydrology, 240(1–2): 131–144.

Llorens P, Domingo F. 2007. Rainfall partitioning by vegetation under Mediterranean conditions. A review of studies in Europe. Journal of Hydrology, 335(1–2): 37–54.

Martinez-Meza E, Whitford W G. 1996. Stemflow, throughfall and channelization of stemflow by roots in three Chihuahuan desert shrubs. Journal of Arid Environments, 32(3): 271–287.

Návar J, Bryan R. 1990. Interception loss and rainfall redistribution by three semi-arid growing shrubs in northeastern Mexico. Journal of Hydrology, 115(1–4): 51–63.

Návar J. 1993. The causes of stemflow variation in three semi-arid growing species of northeastern Mexico. Journal of Hydrology, 145(1–2): 175–190.

Návar J. 2011. Stemflow variation in Mexico's northeastern forest communities: its contribution to soil moisture content and aquifer recharge. Journal of Hydrology, 408(1–2): 35–42.

Nulsen R A, Bligh K J, Baxter I N, et al. 1986. The fate of rainfall in a mallee and heath vegetated catchment in southern Western Australia. Australian Journal of Ecology, 11(4): 361–371.

Pereira F L, Gash J H C, David J S, et al. 2009. Modelling interception loss from evergreen oak Mediterranean savannas: application of a tree-based modelling approach. Agricultural and Forest Meteorology, 149 (3–4), 680–688.

Pressland A J. 1973. Rainfall partitioning by an arid woodland (*Acacia aneura* F. Muell.) in south-western Queensland. Australian Journal of Botany, 21(2): 235–245.

Taniguchi M, Tsujimura M, Tanaka T. 1996. Significance of stemflow in groundwater recharge. 1: evaluation of the stemflow contribution to recharge using a mass balance approach. Hydrological Processes, 10(1): 71–80.

Tromble J. 1988. Water interception by two arid land shrubs. Journal of Arid Environments, 15(2): 65–70.

Voigt G K. 1960. Distribution of rainfall under forest stands. Forest Science, 6(1): 2–10.

Voigt G K, Zwolinski M J. 1964. Absorption of stemflow by bark of young red and white pines. Forest Science, 10(3): 277–282.

Wang X P, Li X R, Xiao H L, et al. 2007. Effects of surface characteristics on infiltration patterns in an arid shrub desert. Hydrology Process, 21(1): 72–79.

Wang X P, Cui Y, Pan Y X, et al. 2008. Effects of rainfall characteristics on infiltration and redistribution patterns in revegetation-stabilized desert ecosystems. Journal of Hydrology, 358(1–2): 134–143.

Weiler M, Flühler H. 2004. Inferring flow types from dye patterns in macroporous soils. Geoderma, 120(1–2): 137–153.

Whitford W G, Anderson J, Rice P M. 1997. Stemflow contribution to the 'fertile island' effect in creosotebush, *Larrea tridentata*. Journal of Arid Environments, 35(3): 451–457.

Wood M K, Jones T L, Vera-Cruz M T. 1998. Rainfall interception by selected plants in the Chihuahuan Desert. Journal of Range Management, 51(1): 91–96.